Journal of
Micro/Nanolithography, MEMS, and MOEMS

SPIEDigitalLibrary.org/jm3

Photoluminescence-enhanced plasmonic substrates fabricated by nanoimprint lithography

Bongseok Choi
Masanobu Iwanaga
Hideki T. Miyazaki
Kazuaki Sakoda
Yoshimasa Sugimoto

SPIE

Photoluminescence-enhanced plasmonic substrates fabricated by nanoimprint lithography

Bongseok Choi,[a] Masanobu Iwanaga,[a,b,*] Hideki T. Miyazaki,[a] Kazuaki Sakoda,[a,c] and Yoshimasa Sugimoto[a]
[a]National Institute for Materials Science (NIMS), Photonic Materials Unit, 1-1 Namiki, Tsukuba 305-0044, Japan
[b]Japan Science and Technology Agency (JST), PRESTO, 4-1-8 Honcho, Kawaguchi 332-0012, Japan
[c]Tsukuba University, Graduate School of Pure and Applied Sciences, 1-1-1 Tennodai, Tsukuba 305-8571, Japan

Abstract. We fabricated large-area stacked complementary plasmonic crystals (SC PICs) by employing ultraviolet nanoimprint lithography. The SC PICs were made on silicon-on-insulator substrates consisting of three layers: the top layer contacting air was a perforated Au film, the bottom layer contacting the buried oxide layer included an Au disk array corresponding to the holes in the top layer, and the middle layer was a Si photonic crystal slab. The SC PICs have prominent resonances in optical wavelengths. It is shown that the fabricated PICs were precise in structure and uniform in their optical properties. We examined the photoluminescence (PL) enhancement of monolayer dye molecules on the SC PIC substrates in the visible range and found large PL enhancements of up to a 100-fold in comparison with dye molecules on nonprocessed Si wafers. [DOI: 10.1117/1.JMM.13.2.023007]

Keywords: plasmonic crystals; plasmonic resonance; photoluminescence enhancement; nanoimprint lithography; large-area fabrication.

Paper 14003P received Jan. 7, 2014; revised manuscript received Apr. 24, 2014; accepted for publication Apr. 30, 2014; published online May 21, 2014.

1 Introduction

Plasmonics that deal with artificial metallic nanostructures is an emerging field to manipulate electromagnetic (EM) waves in the subwavelength dimensions.[1,2] Various applications, such as plasmon-resonance-enhanced spectroscopy, single molecule sensing, and ultrafast processing of signals at optical frequencies along metallic surfaces, are expected. The fundamental aspect of light–matter interaction in locally enhanced EM fields is also attracting interest. Due to the development of fabrication technologies, numerous studies on plasmonics have been conducted, revealing many features of various plasmonic structures, such as nanospheres, nanorods, and nanoantenna. Still, it is a challenge to fabricate precisely controlled metallic nanostructures with areas greater than 1×1 cm^2. Large-area plasmonic substrates are important in making functional plasmon-enhanced sensing practical.[3] There is further demand for better designs and experimental demonstrations of new plasmonic substrates.

It has been reported that the plasmonic resonances mediate enhanced excitation and radiation processes; the resonant modes have even been effectively applied for controlling photoluminescence (PL).[4] Moreover, spectroscopic techniques such as surfaced-enhanced fluorescence have been demonstrated as optical detection methods for bioanalytical applications, wherein the excitation of plasmonic resonances induces strong interactions with the local EM field in close vicinity to metal surfaces.[5] On the other hand, when the molecule is placed directly on the metal surface, the PL intensity in some cases is reduced due to nonradiative decay channels that quench rapid energy transfer to the metal.[6] Therefore, it is important to engineer the radiative coupling between the emitters and the structure in order to enhance the PL extraction efficiency as well as the local EM field-enlarged artificial structures. Most demonstrations of practical sensing substrates involve the use of nanoscale surface structures. A large PL enhancement up to 1340-fold was reported based on bowtie-shaped plasmonic nanoantenna;[7] however, the results showed inhomogeneous enhancement distributions depending on the locations of the molecules. Similarly, metal nanoparticle-based PL enhancement is inhomogeneous due to the limitation of structural reproducibility of the size and local features.[8]

Artificially controlled plasmonic nanostructures at the subwavelength scale are smaller than the available wavelength of illumination. The preparation of such subwavelength plasmonic nanostructures usually involves the use of expensive high-performance equipment for semiconductor mass production. Conventionally, direct-writing electron beam lithography or focused ion-beam techniques are adopted for the fabrication of the nanoscale structures. These techniques are necessary to produce plasmonic resonance in visible regions. However, these methods are slow and expensive, limiting their practical application for the fabrication of large-area surfaces. Given these considerations, nanoimprint lithography (NIL) is considered to be an ideal solution for large-area patterning of nanoscale structures at relatively low cost.[9,10] The NIL technique is based on the direct physical and mechanical deformation of the resist, making it suitable to obtain significantly high resolution, unlike conventional photolithography techniques associated with the light diffraction or scattering. Because of its high resolution, feasibility for mass fabrication, reproducibility, and good uniformity over large surface areas, NIL can be regarded as the most effective nanofabrication technique. Thus far, some studies have demonstrated the fabrication of emission-enhanced substrates using NIL. Nevertheless, most

*Address all correspondence to: Masanobu Iwanaga, E-mail: iwanaga.masanobu@nims.go.jp

studies have mainly focused on the imprint polymer-based PL properties of dielectric substrates.[11,12] Moreover, previous studies on PlCs-based emissions did not demonstrate a significant enhancement because their surrounding dielectric layer of emitters is limited by the effective coupling between the emitters and the excited plasmonic resonances.[13,14] A uniform spectral response of plasmonic resonances without local spot dependence has not been sufficiently demonstrated,[15,16] although higher uniformity of plasmonic resonance on large-area surfaces would enable more quantitative sensing on the substrates.

Figure 1(a) shows the schematic of an SC PlC substrate; the whole view (left) and section view (right) are drawn. The SC structure was conceived to make use of a feature suggested by Babinet's principle,[17] which holds approximately true in actual systems including real metals with finite thickness. The principle implies that two structurally complementary layers have equi-wavelength hetero-resonances, so that when the two layers are closely located, the resonances in each layer couple and form new constructive resonances that are not simple bonding–anti-bonding states.[18,19] The new resonances are featured in the SC structure. Here, we produce large-area silicon-on-insulator (SOI)-based SC PlCs comprised three layers, including two complementary layers in terms of metallic structures. As drawn in Fig. 1(a), the top layer is a perforated thin Au film with 35-nm thickness. The middle layer consists of a perforated Si layer, that is, Si photonic crystal slab with a hexagonal array of air holes; the periodicity was 410.5 nm and the diameter of air holes was 220 nm. The SOI layer was 200 nm in thickness. The bottom layer includes Au disks arrayed in a Si layer of the same thickness as the top layer. Figure 1(b) displays the reflectance (R) calculated by the rigorous coupled-wave approximation method[20] at the normal incidence onto the top xy-plane. Incident polarization was parallel to the x-axis. Several reflection dips are seen in the Au SC PlCs modeling the actual sample (blue line), whereas weak reflection responses are seen for multilayer Au/SOI/BOX on Si wafer (dashed line) that does not include any hole. The permittivity of Au and Si was taken from the literature,[21,22] and that of BOX (or SiO_2) was set to 2.1316.

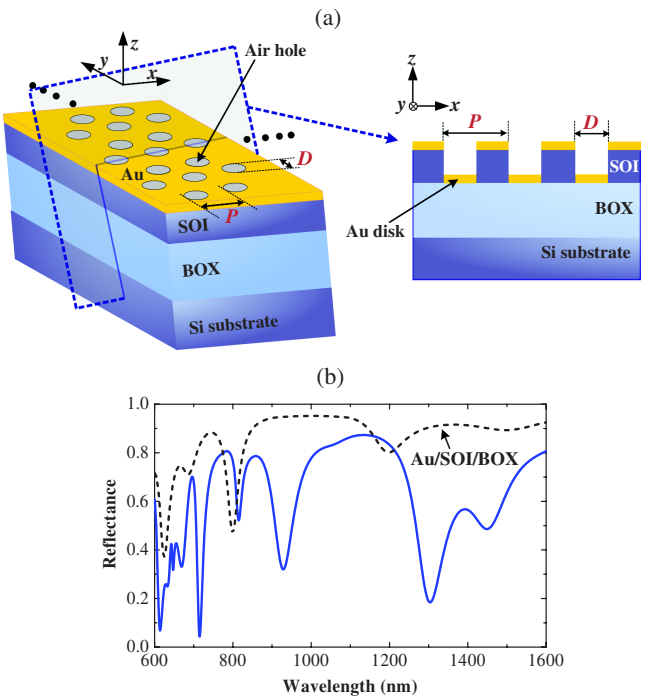

Fig. 1 (a) Schematic of a stacked complementary plasmonic crystal (SC PlC) fabricated in this study. Left: The whole view at an oblique angle. Right: Section view taken at the section indicated at the left. The SC PIC is composed of three layers of SOI; the top layer consists of perforated Au film, the middle layer is perforated Si slab, and the bottom layer includes Au disks. (b) The blue solid curve shows the calculated reflectance (R) spectrum for the SC PIC with periodicity $P = 410.5$ nm, hole diameter $D = 220$ nm, and SOI and BOX (SiO_2) layer thickness of 200 and 400 nm, respectively. Incidence sheds normally on the top xy-plane with polarization parallel to the x-axis in (a). The black dashed curve shows the calculated R spectrum of the Au/SOI/BOX multilayer structure without any hole.

In this paper, we demonstrate the large-area fabrication of Au SC PlC substrates composed of highly uniform nanohole arrays using the ultraviolet (UV)-NIL technique. The surface structures prepared in this study exhibit strongly modified and enhanced emissions compared with the reference Si wafer without Au SC PlCs. The observed enhancement in emissions is attributed to the interactions between the emitter and the plasmonic resonances in the SC PlCs. This experimental study can offer practical PlC substrates that are quite sensitive to luminescent materials.

2 Methods

The fabrication process for Au SC PlCs is illustrated in Fig. 2. The overall mold used was a 33×33 mm^2 quartz stamp with 10×10 mm^2 nanopillar arrays. First, the mold was cleaned by organic solvent pretreatment followed by excimer irradiation with vacuum UV light ($\lambda = 172$ nm) at 150°C. The vacuum UV light cleaning is better than the conventional UV-based cleaning[23] and was done to remove contaminations for the multiple-used mold. The mold surface was subsequently treated with an octadecylsilyl-based monolayer anti-adhesive to improve demolding properties. The anti-adhesion treatment was inevitable in the NIL method using quartz molds because less hydrophobic mold surface adheres to the resist during the imprint press procedure. Note that this step differs from the polymer-mold UV-NIL procedure.[24,25] In the present procedure, the quartz mold was immersed in solutions for 10 min and then gradually taken out of the solution at a constant speed using specifically designed tools. This was performed to ensure a stable and uniform coating. The surface of the mold was subsequently rinsed and then dried at 60°C for 10 min. The used polymer resist (NICT82510, Daicel Chemical Industries, Ltd., Osaka, Japan) was spin-coated with a thickness of approximately 240 nm on a cleaned 50×50 mm^2 SOI wafer and baked at 80°C for 1 min to evaporate residual solvent [Fig. 2(a)]. We used high-precision UV imprint equipment (ST-50, Toshiba Machine Company, Numazu, Japan). The prepared mold and substrate were set, and the mold was then pressed against the substrate at a pressure of 1.5 MPa under the programmed sequential process to control irradiation power and time. The wafer was placed on a 1.5-mm thick Si rubber to avoid partial press distortion during the press process. After imprinting, the mold was removed and the imprinted substrate was baked at 80°C for 10 min [Fig. 2(b)] in order to harden the resist and increase its resistivity for the following dry etching.

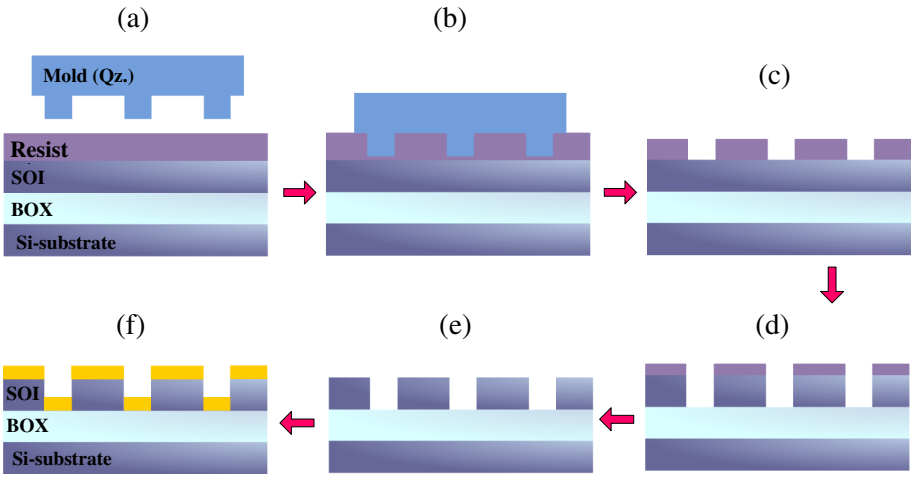

Fig. 2 Fabrication procedure of an Au SC PIC using UV NIL technique. (a) Resist coating, (b) imprint press (stamp and UV irradiation), (c) release and residual removal, (d) anisotropic etching, (e) resist strip, and (f) Au deposition.

The imprinted substrate was etched (not shown in this figure) in the presence of Ar gas to remove the residual or scum [Fig. 2(c)]. Here, achieving a thin layer of residue was highly important for achieving high-aspect-ratio resultant structures. In this study, we optimized the thickness of the resist in the spin-coating step to obtain almost zero imprinted residual. If the thickness was not optimized, resists with thicknesses that are less than half of the mold height were usually ripped away during the demolding step. Thus, it was necessary to optimize the thickness of the resist. The imprinted pattern was subsequently transferred to the SOI layer via anisotropic plasma reactive-ion-etching (RIE) using the Bosch process with SF_6 and C_4F_8 gas for the alternating cycles of etching and passivation, respectively [Fig. 2(d)]. After removal of the resist layer, a 35-nm thick Au film was deposited at an optimized rate of 0.12 nm/s to obtain an Au layer without cracks. The Au was deposited perpendicularly to the air holes using an electron beam evaporation technique [Figs. 2(e) and 2(f)]. Optical characterization of the fabricated Au SC PlCs was performed from the air side.

Figure 3(a) shows the photograph of the resist pattern imprinted onto the substrate in a 10×10 mm^2 area. The thickness of the residual layer was limited to the extremely low thickness of 10 nm, which was close to our target of 10 ± 5 nm [Fig. 3(b)]. The residual layer was subsequently removed via a short Ar plasma-etching treatment. Since the original shape of the quartz mold pattern was slightly tapered, the final profile of the imprinted section was also slightly tapered.

The scanning electron microscopy (SEM) images of the fabricated Au SC PlCs structure are presented in Fig. 3(c). The obtained hole diameter was 225 nm, which is almost the same size as the master mold design. The surface was found to have a uniform hole diameter. The Au thin film was successfully deposited without any cracks during evaporation. The section-view SEM image of Au SC PlCs is shown in Fig. 3(d); 35-nm thick Au layers are clearly observed in the top and bottom layers, and the holes exhibit a slightly bulging rather than a tapered shape. This is attributed to the Bosch Si etching process used in this study to ensure the successful Au profile in the holes. Consequently, we did not observe any isolated Au particles at the middle layer of the SOI walls.

In measuring reflection spectra at the normal incidence, we used a micro-spectroscopy system composed of a 0.4 numerical aperture objective, achromatic imaging lenses, and a charge coupled device (CCD) camera. Reflection spectra of the SC PlCs were measured using incident polarized white light from a tungsten-halogen lamp, a cooled CCD detector array, a multimode fiber, and a spectrometer. The PL measurement was carried out with the same spectroscopy system. The pump laser was a continuous-wave solid state laser with an output wavelength of 532 nm, which was suitable for the dye molecules of Rhodamine 6G (R6G) excitation. The polarization of the laser light was parallel to the x-axis of the Au SC PlCs. The pump laser light through a neutral density filter was focused on a 25-μm diameter spot on the sample surface. In the PL measurements, we observed the PL signals at the spots without an inhomogeneous aggregation of molecules.

To explore emission enhancement, we used R6G dispersed on the fabricated Au SC PlCs substrate. The R6G was melted in methanol at a concentration of 1×10^{-5} M. We also made a reference substrate by dispersing the R6G solution onto Si wafer. After the solvent was entirely evaporated, the PL measurements were carried out at a room temperature. From the concentration of the solution, the average density of R6G on the SC PlCs substrate and the Si wafer was estimated to be 1 molecule/(5×5 nm^2), suggesting that each molecule was isolatedly dispersed.

3 Results and Discussion

Figure 4(a) shows the reflection spectra at normal incidence. The 24 spectra of an Au SC PlC substrate are plotted, measured at different spot with each other. The resulting multiple spectra exhibited significant overlap with each other. The averaged dip minimum corresponds to a reflection efficiency of 13.7% at a wavelength position A (718 nm). The observed results at this position have $\pm 1\%$ reflectance variation for the averaged value. We note that our results were obtained with a temporal fluctuation of the incidence with an approximately 1% variation in light intensity. Therefore, the results of all

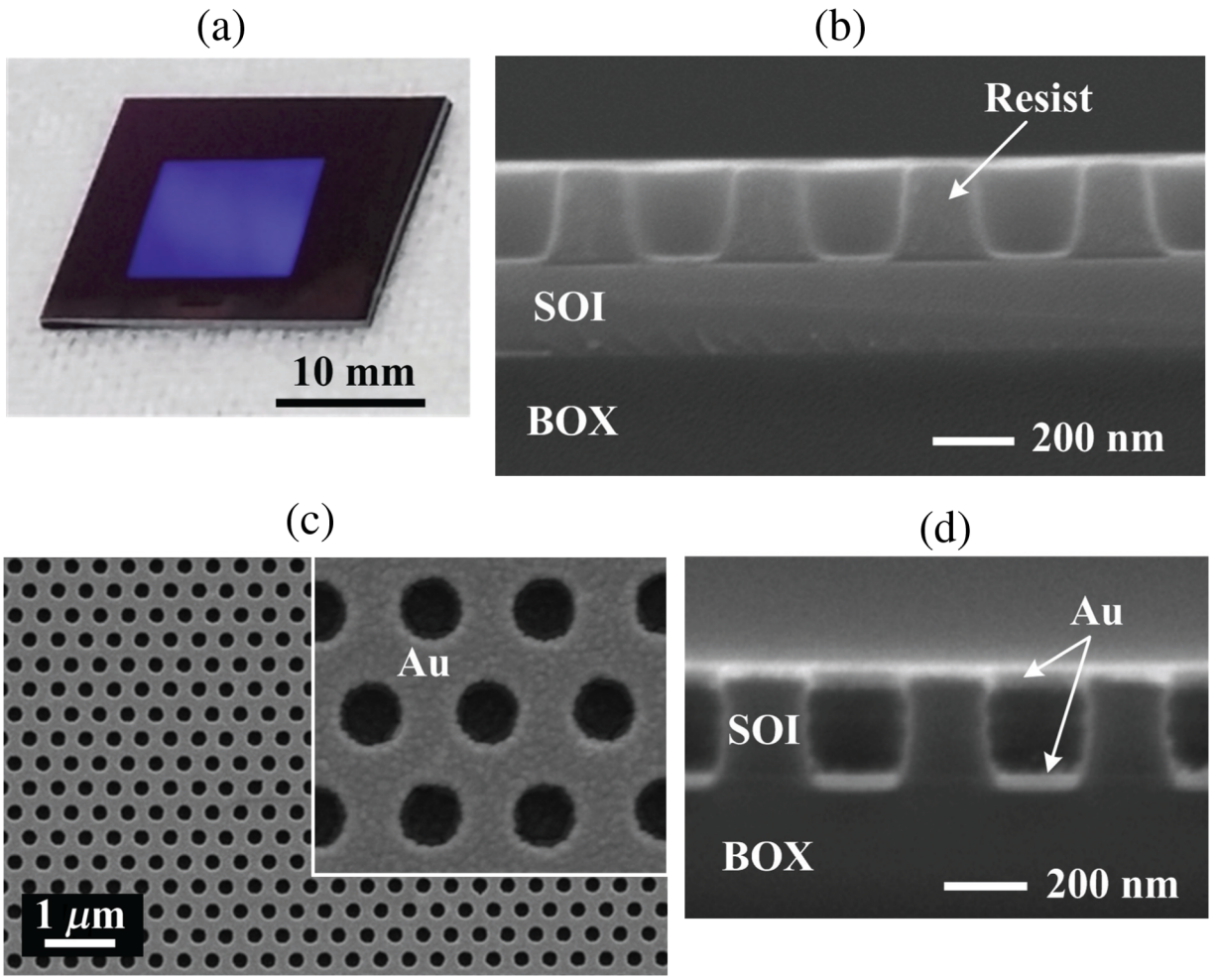

Fig. 3 (a) Photograph of the imprinted substrate with two-dimensional hole array resist patterns. (b) Section-view scanning electron microscopy (SEM) image of the imprinted resist patterns. (c) Top-view SEM images of fabricated Au SC PICs. The SEM image shown in the inset reveals highly uniform shapes of the holes and the Au surface. The hole diameter and lattice constant are 225 and 410.5 nm, respectively. (d) Section-view SEM image of the Au SC PICs clearly indicating the 35-nm-thick Au at the top and bottom of the SOI layer.

24 spots show an almost identical response compared with the results in other studies.[15,16] The reflection spectra imply high spatial uniformity, which is enough to obtain the initially intended optical quality over the whole substrate surface. In addition, the measured result is in good agreement with the calculated reflection efficiency shown in Fig. 1(b). Distinct deep plasmonic resonances were observed at positions A and B, as obtained in the calculation. Because the calculations were implemented based on the ideal model of an Au SC PlC, the observed minor deviations in the reflection efficiency could come from the differences between the model and the actual fabricated structures.

The strong plasmonic resonances observed in the reflection spectra are expected to induce enhanced EM fields around the Au SC PlC, and to significantly enhance emission from the dye molecules. Figure 4(b) shows the measured PL enhancement in an SC PlC substrate. The enhancement factor is the ratio of the PL intensity observed from the dye molecules on an SC PlC substrate to that from molecules adsorbed on a reference substrate (or Si wafer). The inset shown in Fig. 4(b) shows the PL spectrum of the reference Si wafer with a pump power of 250 μW. The peak wavelength was about 610 nm. The PL spectrum from the Au SC PlC is strongly modified when compared with that of the reference substrate. The observed distinct peaks are attributed to the engineered plasmonic resonance effect, and the highest peak at 717 nm indicates a 100-fold increase in the PL intensity for SC PlC compared with the Si substrate. To our knowledge, this is the largest enhancement concerning the highly luminescent R6G molecules. The large enhancement of the PL intensity on the SC PlC can be attributed to the strong interaction between the excited dye molecules and plasmonic resonance modes. The wavelength of the strongly enhanced peaks corresponds to the measured reflection dips. Additionally, another peak at around 800 nm exhibits a 36-fold enhancement. Although the PL of R6G on Si wafer is extremely weak at 800 nm, the highly enhanced PL on the SC PlC substrate is due to the corresponding resonance effect. A slight shift in the peak of the enhancement factor to the reflectance B dip around 800 nm was observed. This shift suggests that the enhanced PL comes from plasmon-molecule coupled states and will be studied in detail by clarifying the plasmon resonance. In the experimental conditions of this study, the dye

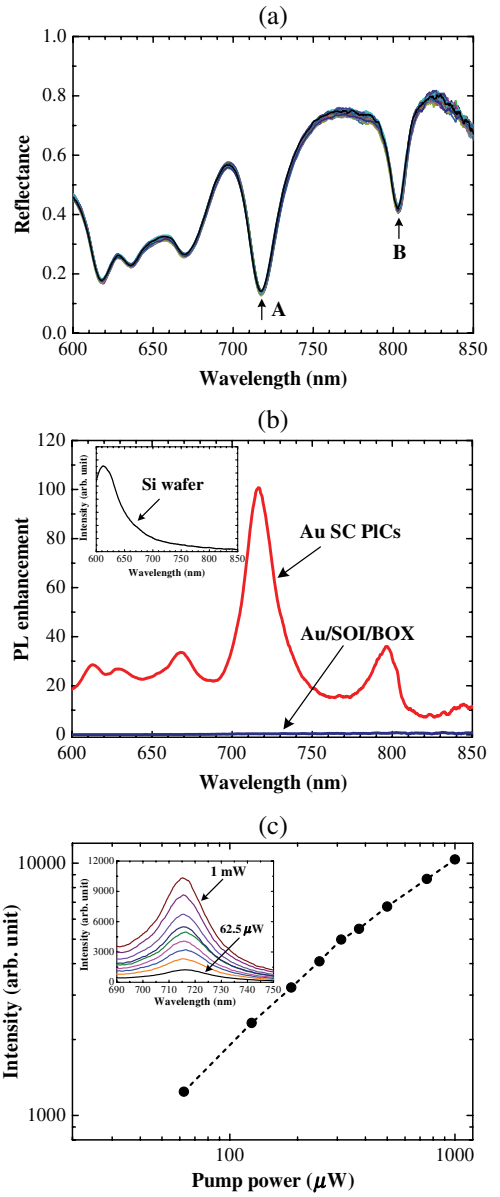

Fig. 4 (a) Measured reflection spectra of the fabricated Au SC PlCs at the normal incidence. Twenty-four spectra are overlaid. (b) Photoluminescence (PL) enhancement of the fabricated Au SC PlCs and Au/SOI/BOX structure on the same substrate. The inset shows the PL spectrum of R6G on the nonprocessed Si wafer. (c) PL intensity at 717 nm, plotted as a function of the pump power. The inset shows the corresponding PL spectra. The laser spot on the sample had a diameter of 25 μm.

molecules were isolatedly dispersed on the substrates; therefore, the enhancement factor is an averaged value over the excitation light spot.

On the other hand, PL enhancement in the order of unity was observed for the R6G molecules dispersed on the Au/SOI/BOX multilayer on the same substrate with SC PlC. The Au/SOI/BOX multilayer does not have so large an EM field due to its simple flat structure; the reflection spectrum is shown in Fig. 1(b). In this case, the reduction of the PL intensity due to quenching on the metal surface may not be negligible.[26] Figure 4(c) presents the pump power dependence PL intensities at 717 nm for Au SC PlC to verify that our PL measurements were performed within a linear response regime of pump intensity. The PL intensity depends almost linearly on the lower pump power (<300 μW). However, when the pump power exceeds a certain critical range, the peak intensity decreases and exhibits a nonlinear dependence, suggesting a photo-breaching effect of the dye molecules.

The emission properties presented here correspond to the resonance response over a large surface structure. One of the meaningful applications of the SC PlC substrates is surface-enhanced Raman scattering[27] because the Au SC PlCs can offer several definite resonant modes in the visible range of interest.

4 Conclusions

In this paper, the PL-enhanced large-area two-dimensional Au SC PlCs using the UV NIL technique combined with RIE and metal deposition are demonstrated. The observed PL intensity of the fabricated structure with R6G was significantly increased by two-orders of magnitude compared with the PL intensity on a reference Si wafer. The three-layered PlCs with hole arrays were precisely fabricated over the substrate in 10×10 mm^2 areas. The fabricated substrate showed deep plasmonic resonances in the measured reflection spectra for visible frequency range. The high-optical uniformity of the fabricated structures is also confirmed by tens of reflection measurements. The optical uniformity suggests that the nanoimprint fabrication process adopted here can be applied to the production of high-quality surface engineered substrates for optical sensing.

Acknowledgments

This study was supported by a Grant-in-Aid for Scientific Research on Innovative Areas from the Japanese Ministry of Education, Culture, Sports, Science and Technology (Grant No. 22109007). The authors would like to thank M. Nakao, T. Kasaya, and T. Mano for technical support, and are grateful to Nippon Soda Co., Ltd. for offering the anti-adhesion coating materials. This work was also supported in part by the NanoIntegration Foundry, Low Carbon Research Network in NIMS. M.I. acknowledges Cyberscience center, Tohoku University, and HPCI System Research Project (ID: hp120066), Japan for supporting numerical implementations.

References

1. E. Ozbay, "Plasmonics: merging photonics and electronics at nanoscale dimensions," *Science* **311**(5758), 189–193 (2006).
2. J. A. Schuller et al., "Plasmonics for extreme light concentration and manipulation," *Nat. Mater.* **9**(3), 193–204 (2010).
3. K. A. Willets and R. P. Van Duyne, "Localized surface plasmon resonance spectroscopy and sensing," *Annu. Rev. Phys. Chem.* **58**(1), 267–297 (2007).
4. A. M. Glass et al., "Interaction of metal particles with adsorbed dye molecules: absorption and luminescence," *Opt. Lett.* **5**(9), 368–370 (1980).
5. F. Tam et al., "Plasmonic enhancement of molecular fluorescence," *Nano Lett.* **7**(2), 496–501 (2007).
6. P. Anger, P. Bharadwaj, and L. Nobotny, "Enhancement and quenching of single-molecule fluorescence," *Phys. Rev. Lett.* **96**(11), 113002 (2006).
7. A. Kinkhabwala et al., "Large single-molecule fluorescence enhancements produced by a bowtie nanoantenna," *Nat. Photonics* **3**(11), 654–657 (2009).
8. K. Ray, R. Badugu, and J. R. Lakowicz, "Distance-dependent metal-enhanced fluorescence from Langmuir-Blodgett monolayers of alkyl-NBD dervatives on silver island films," *Langmuir* **22**(20), 8374–8378 (2006).

9. S. Y. Chou, P. R. Krauss, and P. J. Renstrom, "Imprint of sub-25 nm vias trenches in polymer," *Appl. Phys. Lett.* **67**(21), 3114–3116 (1995).
10. L. J. Guo, "Nanoimprint lithography: methods and materials requirements," *Adv. Mater.* **19**(4), 495–513 (2007).
11. E. B. Namdas et al., "Low thresholds in polymer lasers on conductive substrates by distributed feedback nanoimprinting: progress toward electrically pumped plastic lasers," *Adv. Mater.* **21**(7), 799–802 (2009).
12. V. Reboud et al., "Lasing in nanoimprinted two-dimensional photonic crystal band-edge lasers," *Appl. Phys. Lett.* **102**(7), 073101 (2013).
13. G. Vecchi, V. Giannini, and J. Gómez Rivas, "Shaping the fluorescent emission by lattice resonances in plasmonic crystals of nanoantennas," *Phys. Rev. Lett.* **102**(14), 146807 (2009).
14. V. Reboud et al., "Photoluminescence enhancement in nanoimprinted photonic crystals and coupled surface plasmons," *Opt. Express* **15**(12), 7190–7195 (2007).
15. D. Chanda et al., "Large-area flexible 3D optical negative index metamaterial formed by nanotransfer printing," *Nat. Nanotechnol* **6**(6), 402–407 (2011).
16. J. Yao et al., "Functional nanostructured plasmonic materials," *Adv. Mater.* **22**(10), 1102–1110 (2010).
17. F. J. García de Abajo, "Light scattering by particle and hole arrays," *Rev. Mod. Phys.* **79**(4), 1267–1290 (2007).
18. M. Iwanaga, "Subwavelength electromagnetic dynamics in stacked complementary plasmonic crystal slabs," *Opt. Express* **18**(15), 15389–15398 (2010).
19. M. Iwanaga, "Electromagnetic eigenmodes in a stacked complementary plasmonic crystal slab," *Phys. Rev. B* **82**(15), 155402 (2010).
20. L. Li, "New formulation of the Fourier modal method for crossed surface-relief gratings," *J. Opt. Soc. Am. A* **14**(10), 2758–2767 (1997).
21. A. D. Rakić et al., "Optical properties of metallic films for vertical-cavity optoelectronic devices," *Appl. Opt.* **37**(22), 5271–5283 (1998).
22. E. D. Palik, *Handbook of Optical Constants of Solids II*, Academic Press, San Diego (1991).
23. M. Nakao, M. Yamaguchi, and S. Yabu, "Imprinted-mold-cleaning by vacuum ultraviolet light," *J. Nonlinear Opt. Phys. Mater.* **19**(4), 773–779 (2010).
24. M. Bender et al., "High resolution lithography with PDMS molds," *J. Vac. Sci. Technol. B* **22**(6), 3229–3232 (2004).
25. N. Koo et al., "The fabrication of a flexible mold for high resolution soft ultraviolet nanoimprint lithography," *Nanotechnology* **19**(22), 225304 (2008).
26. S. C. Kitson, W. L. Barnes, and J. R. Sambles, "Surface-plasmon energy gaps and photoluminescence," *Phys. Rev. B* **52**(15), 11441–11445 (1995).
27. A. Otto et al., "Surface-enhanced Raman scattering," *J. Phys. Condens. Matter* **4**(5), 1143–1212 (1992).

Bongseok Choi received his PhD degree in 2007 from Nanomechanics Engineering of Tohoku University, Japan. From 2007 to 2011, he was a senior research engineer in Memory Division at Samsung Electronics Co., Ltd. Currently, he is a postdoctoral researcher in the plasmonics group at NIMS. His work and interests involve research and development of optical metamaterials, nanofabrication of plasmonic structures, and photoemission-related photonic devices.

Masanobu Iwanaga received master's and PhD degrees at Kyoto University, Japan, in 2000 and 2003, respectively. Currently, he is a senior researcher at NIMS, working on photonic metamaterials and plasmonics based on original designs by large-scale simulations, the corresponding nanofabrication, and the optical experiment. He was an assistant professor at the Department of Physics, Tohoku University, Japan, from 2003 to 2009 and moved to NIMS at 2009. He was also a JST PRESTO researcher since October 2010 to March 2014.

Hideki T. Miyazaki received his ME and PhD degrees from the University of Tokyo in 1989 and 1999, respectively. From 1989 to 1994, he was with Hamamatsu Photonics, K. K. From 1994 to 1999, he was a research associate at the University of Tokyo and joined the National Research Institute for Metals (currently, NIMS) in 1999. He has been engaged in research on the interaction of wavelength-sized structures with light waves.

Kazuaki Sakoda graduated and obtained his PhD degree from the University of Tokyo, and worked for Hokkaido University as an associate professor before he joined NIMS. He is the director of the Photonic Materials Unit of NIMS and a professor of Graduate School of Pure and Applied Sciences, Tsukuba University. He has been engaged mainly in the theoretical study of optical properties of solids, especially photonic crystals.

Yoshimasa Sugimoto received the BE degree, the ME degree, and the PhD degree in electronic engineering from Shizuoka University, Shizuoka, Japan, in 1978, 1980, and 1996, respectively. In 1980, he joined the Central Research Laboratories, NEC Corporation, Kawasaki. Since 2007, he has been engaged in NIMS, where he is currently developing nanoprocessing technologies of nanophotonic devices.